Effects of normal aging on myelin sheath ultrastructures in the somatic sensorimotor system of rats

FANG XIE[1,2*], PING LIANG[3*], HAN FU[1*], JIU-CONG ZHANG[4] and JUN CHEN[1]

[1]Institute for Biomedical Sciences of Pain, Tangdu Hospital, The Fourth Military Medical University, Xi'an, Shaanxi 710038; [2]Institute of Basic Medical Sciences, Academy of Military Medical Sciences, Beijing 100039; [3]School of Pharmacy, The Fourth Military Medical University, Xi'an, Shaanxi 710032; [4]Department of Gastroenterology, Lanzhou General Hospital of Lanzhou Military Command, Lanzhou, Gansu 730050, P.R. China

Received August 3, 2013; Accepted April 1, 2014

DOI: 10.3892/mmr.2014.2228

Abstract. Previous studies have presented qualitative and quantitative data regarding the morphological changes that occur peripherally in myelin sheaths and nerve fibers of rats during their lifespan. However, studies on ultrastructural features of myelinated fibers (MFs) in the central nervous system (CNS) remain limited. In the present study, morphological analyses of the somatic sensorimotor MFs in rats at time-points between postnatal day 14 and postnatal month (PNM) 26 were conducted using electron microscopy. Significant alterations in the myelin sheath were observed in the sensorimotor system of aging and aged rats, which became aggravated with age. The ultrastructural pattern of myelin lamellae also exhibited age dependence. The transformation of the myelin intraperiod line from complete to incomplete fusion occurred after PNM 5, leading to an expansion of periodicity in myelin lamellae. These pathological changes in the myelin structure occurred very early and showed a significant correlation with age, indicating that myelin was the part of the CNS with the highest susceptibility to the influence of aging, and may be the main target of aging effects. In addition to the myelin breakdown, continued myelin production and remyelination were observed in the aging sensorimotor system, suggesting the presence of endogenous mechanisms of myelin repair.

Correspondence to: Dr Fang Xie, Institute for Biomedical Sciences of Pain, Tangdu Hospital, The Fourth Military Medical University, 1st Xinsi Road, Baqiao, Xi'an, Shaanxi 710038, P.R. China
E-mail: vancoxie@sina.com

*Contributed equally

Key words: myelin sheath, aging, sensorimotor system, electron microscopy

Introduction

It has long been known that the brain governs body functions with feedforward and feedback neuronal signals transmitted through the peripheral nervous system (PNS), while it also regulates its own functions through structural connections among different parts of the central nervous system (CNS) via nerve fibers. Oligodendrocytes form a laminated, lipid-rich wrapping known as a myelin sheath around most nerve fibers in the CNS, which plays an important role as an insulating coating in maintaining the fast salutatory conduction of action potentials along nerve fibers (1-3). In the past century, only a few studies have focused on the structure and function of nerve fibers compared with nerve cell bodies and synapses. However, over the past few years, the myelin sheath and nerve fibers have attracted increasing attention as it has been demonstrated that white matter exhibits activity-dependent plasticity in a certain period of life (4,5) and can actively affect how the brain learns and dysfunctions (2,6).

Several studies (7-11) have found that the changes in the nerve fibers and myelin sheath, which have been suggested to be affected by aging, are likely to be an important factor in the development of age-related cognitive decline in humans and primates. Myelination is highly specialized and one of the major events occurring during the development of the nervous system (1,12). Numerous nerve function deficits appear with age and have been shown to be the consequence of peripheral myelin abnormalities (13-16). Furthermore, age has been indicated to influence the capability of peripheral nerves to regenerate and reinnervate target organs, but with different patterns for motor and sensory nerve fibers (17,18). However, studies on the effect of aging on myelin sheaths have often been based on comparisons of only two experimental groups, whereas the lifespan and the duration of growth periods should be carefully taken into account. The necessity for assessment at multiple time-points in age studies has been highlighted (19-21).

Several quantitative studies have been conducted on the age-dependent morphological changes that occur in the nervous system; however, these studies have primarily focused on the effects of age on peripheral nerve trunks (15,22-25). To date, comprehensive, detailed investigations concerned with myelin sheaths in the CNS remain limited.

The present study was a controlled morphological investigation of the sensorimotor white matter in multiple age groups of male Sprague Dawley rats covering postnatal to aging periods. The spinal posterior/lateral funiculus and pyramidal tract were selected to represent the sensory and motor projection fibers, respectively. Ultrastructural analyses were performed to define the pattern of changes in the myelinated fibers (MFs) that occur with age in normal animals.

Materials and methods

Animals and treatment. Experiments were performed on male Sprague Dawley albino rats [purchased from Laboratory Animal Center of the Fourth Military Medical University, (FMMU), Xi'an, China]. Time-points of postnatal day (PND) 14, postnatal month (PNM) 2, PNM 5, PNM 12, PNM 18 and PNM 26 were selected for analysis. The animals were housed in plastic cages with access to food and water *ad libitum* and maintained under a 12-h light/dark cycle at room temperature (22-26˚C). The experimental protocols were approved by the Institutional Animal Care and Use Committee of the FMMU (Permit no. SCXK2007-007). The present study was performed in accordance with the National Institutes of Health (NIH) Guide for the Care and Use of Laboratory Animals (NIH Publications no. 80-23) revised in 1996.

Electron microscopy examination of somatic nerve fibers. Five rats per group were infused with 2.5% glutaraldehyde and 4% paraformaldehyde in 0.1 M phosphate buffer (pH 7.4) following anesthetization with sodium pentobarbital (80 mg/kg; Sigma-Aldrich, St. Louis, MO, USA). The brain stem and spinal cord were then collected and fixed with 3% glutaraldehyde in 0.1 M phosphate buffer (pH 7.4) overnight at 4˚C. Transverse sections (1 mm) of the spinal cord were prepared using a vibrating DTK-1000 microtome (Dosaka, Kyoto, Japan). The posterior and lateral funiculus, as well as the pyramidal tract, were dissected and cut into small pieces of similar dimensions, prior to underdoing osmification in 1% OsO_4 in 0.1 M sodium cacodylate buffer for 2 h at room temperature and dehydration with an ascending acetone series. The osmicated tissue blocks were further embedded in Epon-812 (Serva, Heidelberg, Germany) and trimmed under a light microscope. Ultrathin sections (50-70 nm) were cut perpendicularly to the axis of the nerve fibers with a diamond knife on an LKB-11800 ultramicrotome (LKB, Uppsala, Sweden) and collected by copper grids (300 mesh). The ultrathin sections stained with uranyl acetate and lead citrate were observed under an electron microscope (EM; Hitachi, Tokyo, Japan) and microphotographs were captured at the same time.

Histopathological evaluation. Morphometric evaluation of the MFs was performed by assessing ≥200 individual MFs from the sets of photographs selected from five rats at each time-point. Only MFs whose contour was completely within each photograph were used. Measurements of myelin sheath thickness, axon and fiber diameters and g-ratio (which was determined by dividing the axon diameter by the fiber diameter) were obtained using Image-Pro Plus software (Media Cybernetics, Silver Spring, MD, USA). The age-related pathological alterations in the myelin sheath were quantified through pathological grading and counting of the fibers using a method that was established in a previous study by our group (26). Damaged MFs were classified into three grades according to the severity and extent of deterioration, and the percentage of damaged nerve fibers was assessed. Grading was performed as follows: I, minor pathological changes, including myelin lamina rarefaction, focal demyelination or vacuolization, with the axon being less affected; II, moderate pathological changes, including myelin lamina reticulation, focal demyelination, vacuolization and axonal changes, such as increased electron density, lipofuscin deposition or glycogen granules; III, more severe pathological changes, including marked myelin damage or disruption accompanied by axonal degeneration and loss.

Statistical analysis. The Shapiro-Wilk normality test was first used to determine which data were normally or non-normally distributed. Normally distributed data are expressed as the mean ± standard error of the mean, while non-normally distributed data are expressed as the median with a maximum and minimum. One-way analysis of variance followed by Fisher's post hoc least significant difference analysis was used for comparisons of the normally distributed data (periodicity of myelin lamellae) between groups. The Kruskal-Wallis H test and Mann-Whitney U test were used for the comparison of non-normally distributed data (g-ratios and the proportions of damaged MFs). $P<0.05$ was considered to indicate a significant difference between values.

Results

Age-related structural alterations in the general morphology of the myelin sheath. Based on the analysis of the structure of the myelin sheath in the posterior funiculus and pyramidal tract, significant age-related alterations were identified in the sensorimotor projection MFs of rats. In the spinal posterior funiculus of the rats, myelination was not fully completed at PND 14, and ~30% of the fibers appeared as unmyelinated axons. The oligodendrocytes of this development period were activated and contained little heterochromatin, which contributed to the comparatively pale appearance of the nuclei of the oligodendrocytes under the EM (Fig. 1A). Myelination was not completed until PNM 2, and nearly all axons were wrapped by an integrated myelin sheath at this time-point. During this period, the level of heterochromatin in the nuclei of the oligodendrocytes increased, which was a typical characteristic of normal oligodendrocytes (Fig. 1B). Significant levels of myelin breakdown occurred in the spinal posterior funiculus of rats at PNM 12, including myelin tubercles, myelin ballooning, the general separation of myelin lamellae and the atrophy and degeneration of axons (Fig. 1C). A comparable but more extensive myelin breakdown was observed in the posterior funiculus of rats at PNM 26. Severe decompaction of lamellae gave the myelin structure a wave-like appearance. The degeneration of several oligodendrocytes and axons was identified by an abnormally high electron density (Fig. 1D).

The age-related changes in the myelin sheath in the pyramidal tract were similar to those in the posterior funiculus. However, compared with the posterior funiculus, the development of the myelin sheath in the pyramidal tract was

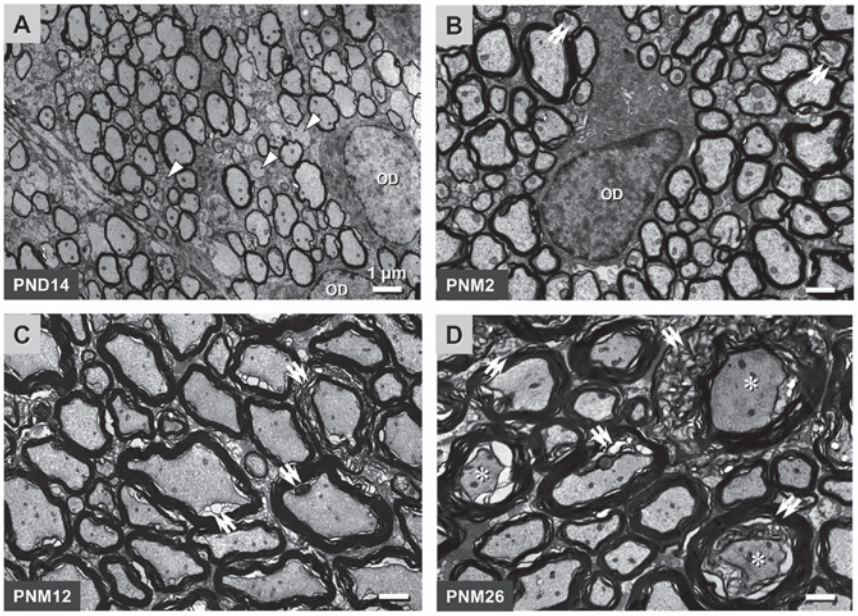


Figure 1. Effects of normal aging on the myelinated fiber structures in the spinal posterior funiculus of rats. (A-D) Electron microscopic photomicrographs were captured from the ultrathin cross-sections of the spinal posterior funiculus of rats at (A) PND 14, (B) PNM 2, (C) PNM 12 and (D) PNM 26 (magnification, x2,500). At PND 14, myelination was not fully completed and several unmyelinated fibers appeared in the spinal posterior funiculus (triangle in A). Significant pathological changes characterized by myelin breakdown or disruption (double arrow in B-D), occurred in aged animals. Axon degeneration (asterisks) was mainly observed at (D) PNM 26 as compared with (A) PND 14 and (B) PNM 2. The nuclei of oligodendrocytes are marked as OD. Scale bar, 1 μm. PND, postnatal day; PNM, postnatal month.

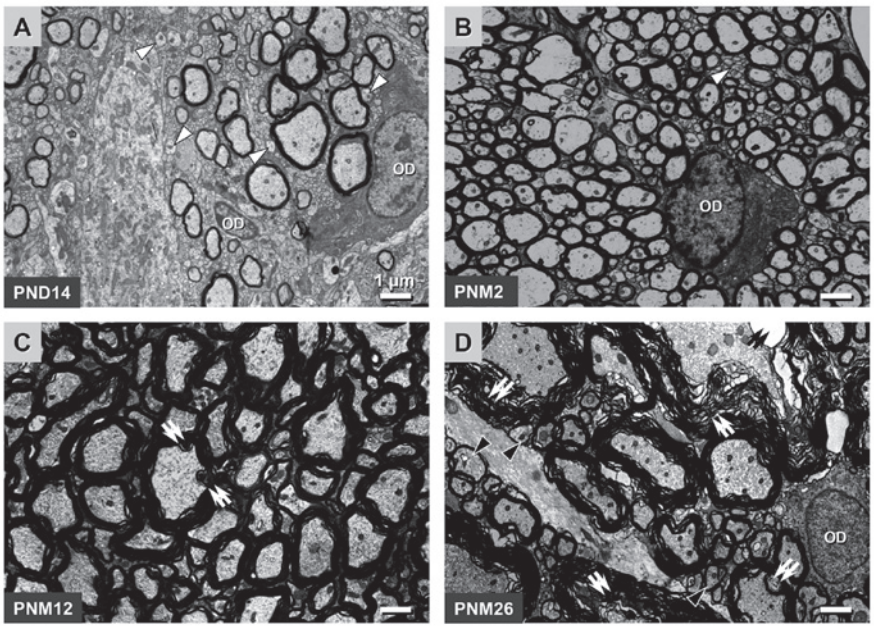


Figure 2. Histopathological evidence shows the age-related neuropathy of myelinated fibers in the pyramidal tract of rats. Electron microscopic photomicrographs show cross-sections of pyramidal tract fibers at (A) PND 14, (B) PNM 2, (C) PNM 12 and (D) PNM 26 (magnification, x2,500). Myelination was not fully completed at PND 14, and several unmyelinated fibers appeared in the pyramidal tract at PND 14 and PNM 2 (white triangles in A and B). Severe pathological changes characterized by myelin breakdown or disruption (white double arrows in C and D) occurred in aged animals. Oligodendrocyte degeneration was rare, while axon degeneration was characterized as axon ballooning (black double arrow in D). Remyelination could be identified by the thinly myelinated fibers in aged rats (black triangles in D). The nuclei of oligodendrocytes are marked as OD. Scale bar, 1 μm; PND, postnatal day; PNM, postnatal month.

moderately delayed. A total of >50% fibers had unmyelinated axons at PND 14 and only a small number of unmyelinated fibers could be observed in the pyramidal tract at PNM 2. Myelin breakdown appeared at PNM 12 and became more aggravated at PNM 26 (Fig. 2A-D).

Quantitative analysis of the age-related structural alterations in the myelin sheath. Using quantitative image analysis tools, myelin thickness, axon diameters and g-ratios were measured in the posterior funiculus and pyramidal tract at PNM 2, 12 and 26. The rightward shift of the peak in the frequency

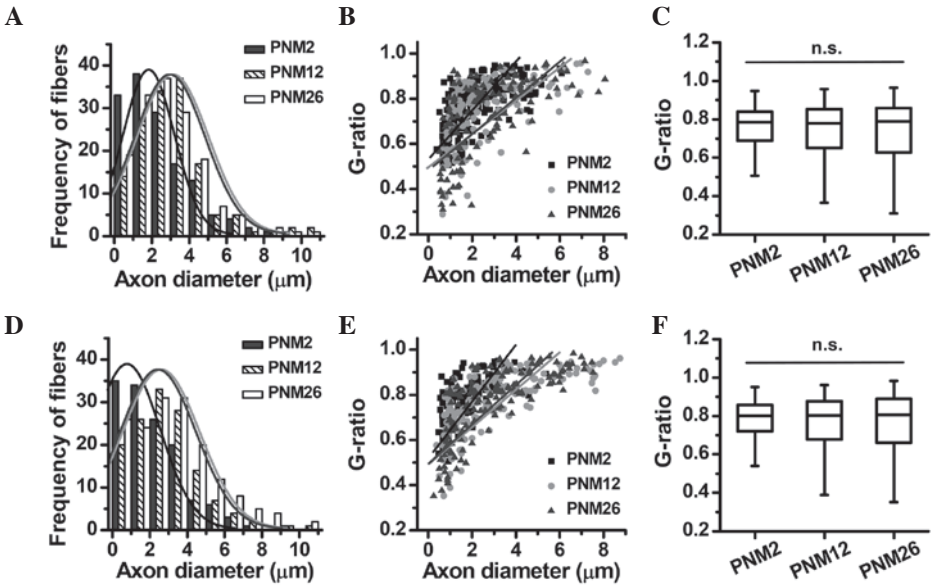


Figure 3. g-ratio is not a suitable parameter to evaluate the integrity of the myelin sheath in normal aging. Age-related changes in axon diameter and g-ratio in the (A-C) spinal posterior funiculus and (D-F) pyramidal tract are shown. g-ratio as a function of axon diameter changed with age in the (B) posterior funiculus and (E) pyramidal tract. Due to enlargements in axon diameters (A and D), the slope rate of fitting lines decreased in rats at PNM 12 and 26 (B and E). (C and F) Comparison of g-ratios in the posterior funiculus and pyramidal tract, respectively, among the three groups. The mid-line in each data box represents the median. Error bars show the maximum and minimum, with the exception of outliers. The graph represents the g-ratios obtained from >200 myelinated fibers (a total of five animals per age). n.s., no significance. PNM, postnatal month.

distribution of axon diameters indicated that the axons were enlarged in the posterior funiculus and pyramidal tract at PNM 12 and 26 (Fig. 3A and D). The g-ratio as a function of axon diameter also changed with increasing age: The slope rate of the g-ratio fitting line was decreased at PNM 12 and 26, while the distribution of g-ratios showed no statistical changes in the posterior funiculus and pyramidal tract among the three age groups (Fig. 3).

The grading classification of the pathological changes in the myelin sheath showed the age dependence of myelin breakdown (Fig. 4A and C). The percentage of nerve fibers with a pathological alteration in the myelin structure increased significantly in the posterior funiculus and pyramidal tract of aging and aged rats; however, the myelin disruption in the pyramidal tract was less severe than that in the spinal posterior funiculus (Fig. 4B and D). The percentage of fibers with myelin disruption reached 37.8 and 28.6% in the posterior funiculus and pyramidal tract at PNM 26, respectively.

Age-related alterations in the ultrastructural pattern of myelin lamellae. Using high-resolution electron microscopy, the ultrastructure of myelin lamellae was observed in the posterior funiculus of rats at PNM 2, 5, and 18. The ultrastructural pattern of myelin lamellae also showed significant age-related alterations. The extracellular surface of the myelin membrane fused completely at the time of myelination (PNM 2), which made the intraperiod lines (IPLs) appear as single, thin lines similar to the major dense lines (MDLs) under the EM. It was difficult to distinguish between the MDLs and IPLs in the high-magnification images at PNM 2 (Fig. 5a and Ab). The normal, double-line appearance of the IPLs was observed in myelin lamellae of rats at PNM 5 and thereafter, which indicated incomplete fusion of the IPLs at these periods (Fig. 5B and C). As shown in Fig. 6, at PNM 26, several IPLs opened to form cavities between the myelin lamellae in the spinal lateral funiculus (Fig. 6B).

The assessment of the periodicity of the myelin lamellae indicated that the distance between adjoining MDLs and IPLs increased statistically with age. The periodicity of the MDLs was elevated from 13.09 nm at PNM 2 to 15.23 nm at PNM 18, while the periodicity of the IPLs increased from 12.88 to 14.98 nm (Fig. 5D).

Evidence of continued myelin production and remyelination in the CNS of aged rats. In the CNS of rats at PNM 18 and 26, the myelin sheath of certain fibers was observed to be overly thick. These fibers had ≥20 myelin lamellae; however, the axon diameters were not expanded accordingly, which led to g-ratios of <0.4 in overly thick MFs. In several cases, this overly thick myelin contained circumferential splits, giving the sheath the appearance of an inner set of compact lamellae surrounded by an outer separated loose set (Fig. 6A). Under the EM at high magnification, the outer set of myelin lamellae had a similar ultrastructural pattern to that observed in the CNS of rats at PNM 5 and 18. The IPLs in the outer myelin sheath fused incompletely, showing the typical double-line pattern of aging myelin lamellae, while the IPLs in the inner compact myelin sheath fused completely to form single lines. This pattern was similar to the ultrastructural pattern of myelin lamellae in the posterior funiculus at PNM 2 (Fig. 6B).

By comparing the myelin structure in rats during the aging and developmental periods, it was observed that certain myelin sheath samples of the posterior and lateral funiculus in the aging period exhibited similar characteristics to those in the developmental period (Fig. 7). For example, certain MFs in aging rats CNS had thin myelin sheaths, a higher g-ratio, fewer myelin lamellae and a large inner tongue process of the myelin sheath, which were typical characteristics of MFs

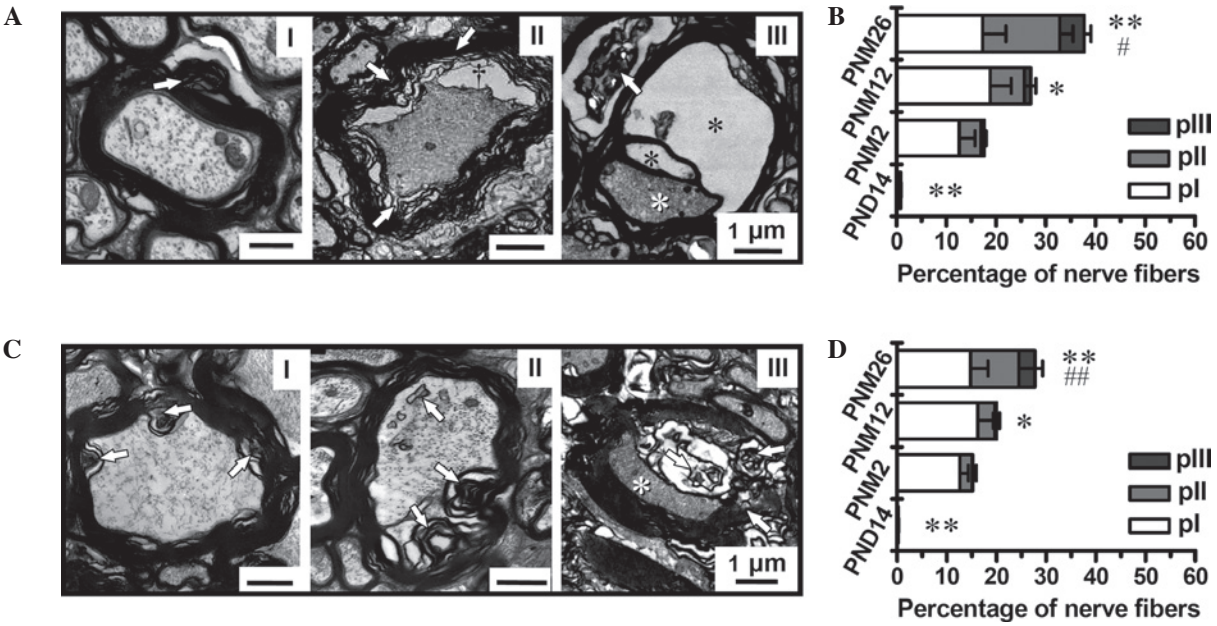


Figure 4. Grading classification of pathological changes and quantitative analysis of MFs in aged (A and B) posterior funiculus and (C and D) pyramidal tract (magnification, x4,000). (A and C) Grading classification of pathological changes in the posterior funiculus and pyramidal tract of rats between PND 14 and PNM 26: I, Slight pathological changes in the myelin sheath, shown as focal myelin damage or vacuolization with the axon being less affected; II, moderate pathological changes in the myelin sheath, shown as more intensive myelin damage featured by large lamina decompaction, vacuolization and intra-axonal changes (increased electron density, lipofuscin deposition and glycogen granules); III, the most severe pathological changes in the myelin sheath and axons, shown as dramatic myelin damage or disruption that were accompanied by axonal degeneration and loss (white asterisks). Black asterisks indicate ballooning of the myelin sheath. (B and D) Proportions of MFs with different pathologically-classified grades (pI-III) in the posterior funiculus and pyramidal tract, respectively. Scale bars, 1 μm. *P<0.05 and **P<0.01 versus PNM 2; $^{\#}$P<0.05 and $^{\#\#}$P<0.01 versus PNM 12. Results in B and D are presented as the mean ± standard error of the mean. MF, myelinated fiber; PND, postnatal day; PNM, postnatal month.

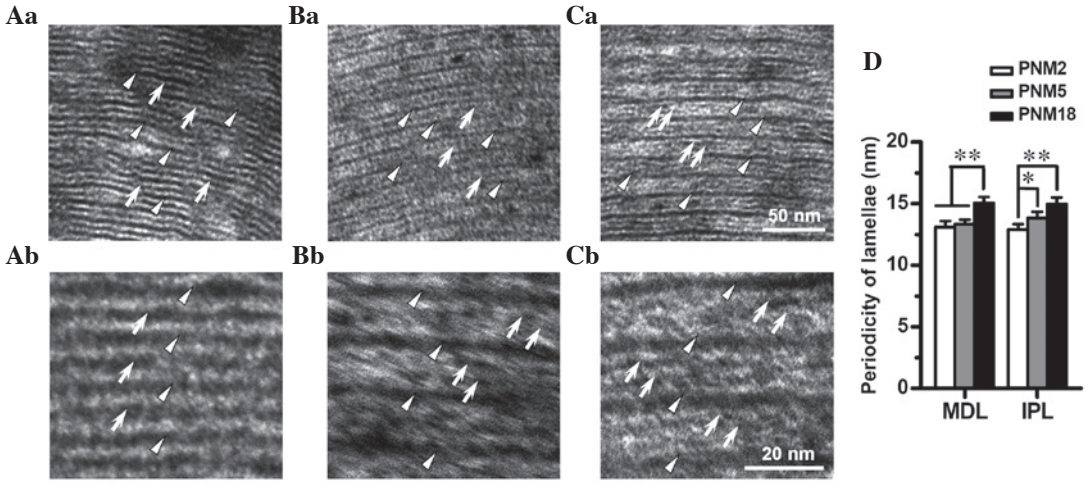


Figure 5. Age-related alterations in the ultrastructure of myelin lamellae in the spinal posterior funiculus. Electron microscopic photomicrographs show the ultrastructure of the posterior funiculus myelin lamellae at (Aa and Ab) PNM 2, (Ba and Bb) PNM 5 and (Ca and Cb) PNM 18 (Aa-Ca magnification, x80,000; Ab-Cb magnification, x160,000). IPLs (white arrows) are fused as a less dark line (Aa), and could hardly be distinguished from MDLs (white triangles) at a high magnification (Ab) in rats at PNM 2. The ordinary double-line appearance of the IPLs was observed at PNM 5 (Ba and Bb). Double-line IPLs were more obvious in the myelin sheath of the posterior funiculus at PNM 18 (Cb) and were clear even at a low magnification (Ca). (D) Bar chart of the periodicity of myelin lamellae in the posterior funiculus of young and aged rats. (Aa-Ca) Scale bars, 50 nm; (Ab-Cb) scale bars, 20 nm; *P<0.05 and **P<0.01. Results in D are presented as the mean ± standard error of the mean. PNM, postnatal month; IPL, intraperiod line; MDL, major dense line.

in the developmental process (Fig. 7A and B). Certain other nerve fibers in aged rats had myelin sheaths that were separated by oligodendrocyte cytoplasmic components between compacted myelin lamellae, appearing as a multi-layer concentric structure. This phenomenon was also common in MFs of rats at the development stage (Fig. 7C and D). These results suggested the existence of continued myelin production and remyelination in the spinal posterior and lateral funiculus of aged rats.

Discussion

The assessment of the g-ratio is a conventional quantitative method used to detect the myelinating capacity of

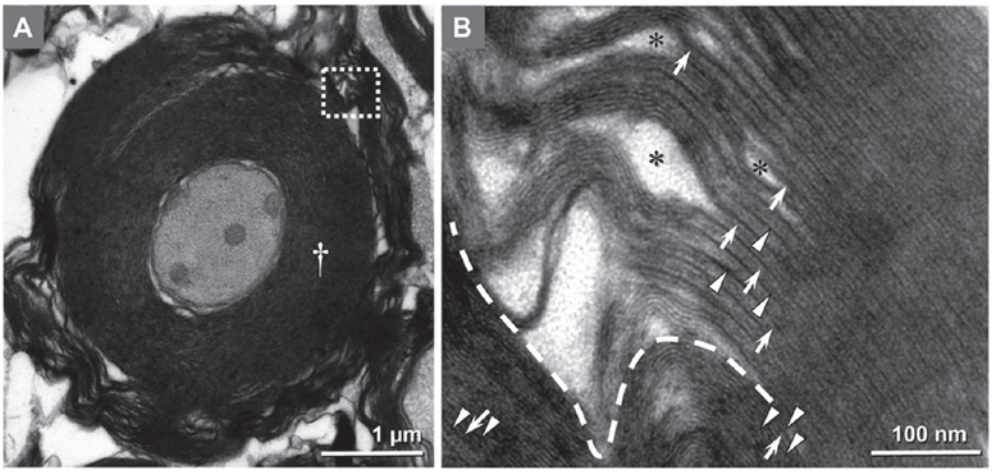


Figure 6. The over-incrassate myelin sheath and different patterns in the ultrastructure of intra- and extra-lamellae indicated the continued production of myelin in aging. (A) Cross-section of a myelinated fiber in the lateral funiculus of rats at PNM 26, as observed under the electron microscope (magnification, x8,000). The over-incrassate myelin sheath (white cross) decreased the g-ratio to 0.374. Of note, a gap appeared between the intra- and extra-myelin structures. (B) High-magnification (magnification, x80,000) image of the white square in A. Patterns in the ultrastructure of intra- and extra-myelin lamellae are significantly different. Gaps between IPLs are marked as black asterisks. The white triangles and arrows indicate MDLs and IPLs, respectively. Scale bar in (A), 1 μm and (B), 100 nm. PNM, postnatal month; IPL, intraperiod line; MDL, major dense line.

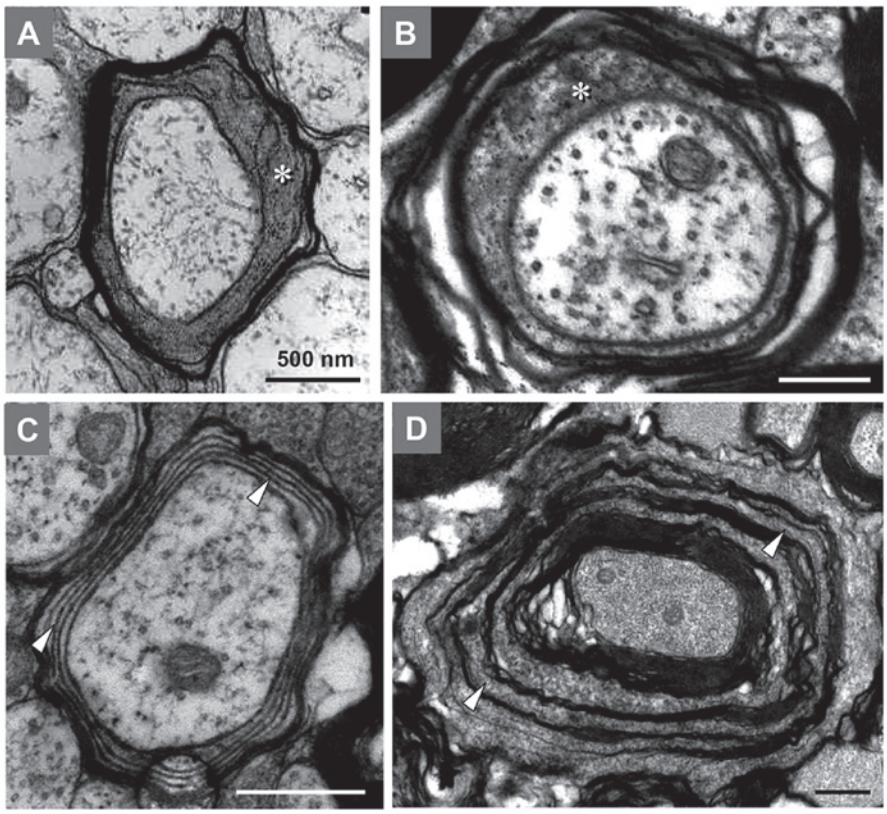


Figure 7. Similar patterns of remyelination in aging and myelination in development. Photomicrographs obtained using an electron microscope (magnification, x15,000) show the cross-section of a myelinated fiber in the posterior funiculus of rats at (A) PND 7 and (B) PNM 18 and in the lateral funiculus at (C) PND 14 and (D) PNM 26. (A and B) Few myelin lamellae and the large inner tongue process (asterisks) may be observed. (C and D) The similarity of myelination and remyelination of lateral funiculus fibers in developing and aging rats may be observed, including the compact myelin lamellae, which were separated by oligodendrocyte plasma (triangles). Scale bars, 500 nm. PND, postnatal day; PNM, postnatal month.

oligodendrocytes in the CNS and Schwann cells in the PNS. Furthermore, this technique has been widely used to evaluate the effects of drugs or gene mutation on myelination (27-29). In these studies, an increase in the g-ratio was generally considered to indicate a decline in myelinating capacity, while a decrease in the g-ratio was suggested to indicate increased myelination. Variations in the g-ratio of the animals and age-matched controls were identified as a leftward or rightward shifting of the g-ratio fitting line to axon diameters. However, when this method was used to evaluate the effects

of aging on rat myelin integrity, several problems appeared. In contrast to previous studies, which indicated no change in the visual cortex axon diameters in monkeys with age (9), the present study suggested that axon diameters increase in the sensorimotor projection fibers of aging and aged rats (Fig. 3A and D). This inconsistency may be due to differences between animal species. The age-related enlargement of axon diameters disturbed the g-ratio as a function of axon diameter, which caused a clockwise rotation of the fitting line rather than a parallel shift. However, age-related myelin breakdown was more complex than simple dysmyelination or demyelination. Certain demyelinated fibers had an increased g-ratio, while fibers with decompacted myelin had a decreased g-ratio. Therefore, the median g-ratio value in aging could be maintained at the same level as that in young rats (Fig. 3C and E). Accordingly, the conventional method of assessing the g-ratio was not suitable for evaluating the integrity of the myelin sheath in normal aging.

Using the method for the pathological grading and counting of fibers established in a previous study conducted by our group (26), the degree of myelin disruption in the sensorimotor system of aging rats was successfully quantified, and it was found that the pathological alterations in the myelin sheath were significantly age-dependent. At only PNM 2, the myelin sheath in the sensorimotor projection fibers of rats began to show minor pathological changes. More significant pathological alterations were identified in rats at PNM 12, which became more severe in the sensorimotor system of older rats. A similar age-related myelin breakdown has also been reported in the PNS of rats (14,15,30,31), where marked abnormalities in the myelin sheath of peripheral nerves were observed at 12 and 18 months of age.

Peters *et al* (11,32,33) defined two types of the most common age-related morphological alterations in the myelin sheath in their studies on the CNS of monkeys: i) Accumulation of pockets of dense cytoplasm between splits of the lamellae at the MDL; and ii) fluid-filled cavities that occupy splits in the IPL of the sheath. The cavities formed by the IPL opening of the myelin sheath were also able to be observed in the posterior funiculus of aged rats in the present study (Figs. 4A and 6B); however, the pockets of dense cytoplasm in the MDL were rare in the CNS of aged rats. The most common pathological changes in the myelin sheath in the present study were a wave-like decompaction of myelin lamellae and an atrophy of axons (Figs. 1, 2 and 4). Other structural alterations included sclerosis of myelin, splits between myelin lamellae, ballooning of axons and localized demyelination. Compared with other studies (15,18,30,34), the diversity in myelin breakdown in the CNS was not as high as that in the PNS of rats. These results suggested that there were differences in age-related myelin breakdown among different species and locations.

Another notable finding of the present study was that the ultrastructural pattern of the myelin lamellae was not inflexible with age (Fig. 5). Furthermore, the extracellular surface of the myelin membrane fused completely at the exact time of myelination, which made the IPL appear as a single thin line under the EM. The ordinary double-line appearance of the IPL was not observed until PNM 5. This result indicated that the stability of the myelin IPL in the sensorimotor system of rats decreased with age and that the decreased stability of the IPL in aging may be the structural basis of age-related myelin breakdown. The mechanism underlying this age-related change in the IPL remains to be elucidated; however, considering the important roles of myelin-associated proteins in maintaining the integrity of myelin lamellae, it is assumed that this is likely to be linked with the alterations in myelin proteins. Further studies are required to explore the correlation between age-related changes in the IPL ultrastructure and age-dependent alterations in myelin proteins.

Besides the pathological disruption of the myelin sheath, continued myelin production and remyelination were also identified in the CNS of aging rats (Figs. 6 and 7). Two types of abnormal myelin sheath were identified by Peters *et al* (8,32,33) and Luebke *et al* (35) as evidence of continued myelin production in the CNS of aged monkeys: i) An overly thick myelin sheath with >20 lamellae; and ii) redundant myelin which was overly large in relation to the size of the enclosed axon. In the present study, redundant myelin was only observed in the PNS of aged rats (data not shown), while an overly thick myelin sheath was common in the CNS of aged rats (Fig. 6). The same thickened myelin sheath has also been observed in the paranodal junction of MFs in the corpus callosum of aged rats (36). Of note, two distinct patterns in the lamellae existed in one single myelin sheath (Fig. 6B). This difference between the inner and outer set of lamellae may be a novel piece of evidence of continued myelin production in the CNS of aging rats, and may imply that myelin repair during the aging period occurs at the adaxonal membrane of myelin-forming cells.

The increased frequency of the profiles of paranodes under the EM has been suggested to evidence remyelination in the CNS of aged monkeys (37). In the present study, too few paranodes were found for statistic analysis; however, by comparing the myelin sheaths in the aging and developing sensorimotor systems of rats, similar structural patterns between these two age periods were identified. This similarity may be a novel piece of evidence for the existence of remyelination in the CNS of aged rats.

In conclusion, the present study provides a detailed description of the age-related changes in the myelin sheath in sensorimotor projection fibers throughout the lifespan of rats. Marked alterations in the myelin sheath were observed in the sensorimotor system of aging and aged rats, which became aggravated with age, resulting in the appearance of a wave-like decompaction of myelin lamellae, sclerosis of myelin, splits between myelin lamellae, ballooning of axons and localized demyelination. The ultrastructural pattern of myelin lamellae also exhibited age dependence. The transformation of myelin IPL from complete to incomplete fusion occurred after PNM 5, leading to the expansion of periodicity in myelin lamellae. These pathological changes in the myelin structure occurred very early and showed a significant correlation with age, indicating that myelin was the most susceptible part of the nervous system to the influence of aging, and myelin may be the major target of aging effects. Besides myelin breakdown, continued myelin production and remyelination also existed in the aging sensorimotor system, which suggested the presence of endogenous mechanisms of myelin repair. This repair may provide a basis for future drug research and development on the modulation of myelin protection.

Acknowledgements

The authors are grateful to X.L. Wang and Y. Yang for specific pathogen free animal supplies and their collaboration. The present study was supported by grants from the Major State Basic Research Development Program of China (973 Program) (nos. 2011CB504100 and 2013BAI04B04) and the National Natural Science Foundation of China (no. 81171049).

References

1. Asou H, Hamada K and Sakota T: Visualization of a single myelination process of an oligodendrocyte in culture by video microscopy. Cell Struct Funct 20: 59-70, 1995.
2. Fields RD: White matter matters. Sci Am 298: 42-49, 2008.
3. Waxman SG: Conduction in myelinated, unmyelinated, and demyelinated fibers. Arch Neurol 34: 585-589, 1977.
4. Bengtsson SL, Nagy Z, Skare S, Forsman L, Forssberg H and Ullén F: Extensive piano practicing has regionally specific effects on white matter development. Nat Neurosci 8: 1148-1150, 2005.
5. Fields RD: Myelination: an overlooked mechanism of synaptic plasticity? Neuroscientist 11: 528-531, 2005.
6. Bartzokis G: Age-related myelin breakdown: a development modal of cognitive decline and Alzheimer's disease. Neurobiol Aging 25: 5-18, 2004.
7. Albert M: Neuropsychological and neurophysiological changes in healthy adult humans across the age range. Neurobiol Aging 14: 623-625, 1993.
8. Peters A: The effects of normal aging on myelin and nerve fibers: a review. J Neurocytol 31: 581-593, 2002.
9. Peters A, Sethares C and Killiany RJ: Effects of age on the thickness of myelin sheaths in monkey primary visual cortex. J Comp Neurol 435: 241-248, 2001.
10. Hinman JD and Abraham CR: What's behind the decline? The role of white matter in brain aging. Neurochem Res 32: 2023-2031, 2007.
11. Peters A and Kemper T: A review of the structal alterations in the cerebral hemispheres of the aging rhesus monkey. Neurobiol Aging 33: 2357-2372, 2012.
12. Black JA, Foster RE and Waxman SG: Rat optic nerve: freeze-fracture studies during development of myelinated axons. Brain Res 250: 1-20, 1982.
13. Chase MH, Engelhardt JK, Adinolfi AM and Chirwa SS: Age-dependent changes in cat masseter nerve: an electrophysiological and morphological study. Brain Res 586: 279-288, 1992.
14. Majeed SK: Survey on spontaneous peripheral neuropathy in aging rats. Arzneimittelforschung 42: 986-990, 1992.
15. Sharma AK, Bajada S and Thomas PK: Age changes in the tibial and plantar nerves of the rat. J Anat 130: 417-428, 1980.
16. Stanmore A, Bradbury S and Weddell AG: A quantitative study of peripheral nerve fibres in the mouse following the administration of drugs. 1. Age changes in untreated CBA mice from 3 to 21 months of age. J Anat 127: 101-115, 1978.
17. Navarro X and Kennedy WR: The effects of ageing on regeneration and sprouting of unmyelinated axons. In: Peripheral Nerve Changes in the Elderly. New Issues in Neurosciences. Thomas PK (ed). Vol 1. Wiley & Sons, New York, NY, pp125-134, 1989.
18. Verdú E, Butí M and Navarro X: Functional changes of the peripheral nervous system with aging in the mouse. Neurobiol Aging 17: 73-77, 1996.
19. Coleman P, Finch C and Joseph J: The need for multiple time points in aging studies. Neurobiol Aging 25: 3-4, 2004.
20. Jernigan TL and Fennema-Notestine C: White matter mapping is needed. Neurobiol Aging 25: 37-39, 2004.
21. Coleman PD: How old is old? Neurobiol Aging 25: 1, 2004.
22. Ceballos D, Cuadras J, Verdú E and Navarro X: Morphometric and ultrastructural changes with ageing in mouse peripheral nerve. J Anat 195: 563-576, 1999.
23. Behse F: Morphometric studies on the human sural nerve. Acta Neurol Scand Suppl 132: 1-38, 1990.
24. Arbuthnott ER, Boyd IA and Kalu KU: Ultrastructural dimensions of myelinated peripheral nerve fibres in the cat and their relation to conduction velocity. J Physiol 308: 125-157, 1980.
25. Friede RL and Samorajski T: Myelin formation in the sciatic nerve of the rat. A quantitative electron microscopic, histochemical and radioautographic study. J Neuropathol Exp Neurol 27: 546-570, 1968.
26. Xie F, Fu H, Hou JF, Jiao K, Costigan M and Chen J: High energy diets-induced metabolic and prediabetic painful polyneuropathy in rats. PLoS One 8: e57427, 2013.
27. Fancy SP, Baranzini SE, Zhao C, *et al*: Dysregulation of the Wnt pathway inhibits timely myelination and remyelination in the mammalian CNS. Genes Dev 23: 1571-1585, 2009.
28. La Marca R, Cerri F, Horiuchi K, *et al*: TACE (ADAM17) inhibits Schwann cell myelination. Nat Neurosci 14: 857-865, 2011.
29. Makinodan M, Rosen KM, Ito S and Corfas G: A critical period for social experience-dependent oligodendrocyte maturation and myelination. Science 337: 1357-1360, 2012.
30. Knox CA, Kokmen E and Dyck PJ: Morphometric alteration of rat myelinated fibers with aging. J Neuropathol Exp Neurol 48: 119-139, 1989.
31. Thomas PK, King RH and Sharma AK: Changes with age in the peripheral nerves of the rat. An ultrastructural study. Acta Neuropathol 52: 1-6, 1980.
32. Peters A: The effects of normal aging on nerve fibers and neuroglia in the central nervous system. In: Brain Aging: Models, Methods, and Mechanisms. Riddle DR (ed). CRC Press, Boca Raton, FL, pp97-125, 2007.
33. Peters A: The effects of normal aging on myelinated nerve fibers in monkey central nervous system. Front Neuroanat 3: 11, 2009.
34. Krinke G, Froehlich E, Herrmann M, *et al*: Adjustment of the myelin sheath to axonal atrophy in the rat spinal root by the formation of infolded myelin loops. Acta Anat (Basel) 131: 182-187, 1988.
35. Luebke J, Barbas H and Peters A: Effects of normal aging on prefrontal area 46 in the rhesus monkey. Brain Res Rev 62: 212-232, 2010.
36. Sugiyama I, Tanaka K, Akita M, Yoshida K, Kawase T and Asou H: Ultrastructural analysis of the paranodal junction of myelinated fibers in 31-month-old-rats. J Neurosci Res 70: 309-317, 2002.
37. Peters A and Sethares C: Is there remyelination during aging of the primate central nervous system? J Comp Neurol 460: 238-254, 2003.